

ORGANOMETALLICS

Volume 9, Number 4, April 1990

© Copyright 1990
American Chemical Society

Metal π -Complexes of Benzene Derivatives. 34.¹ Tetraphenylsilane as a Chelating Ligand: Synthesis, Structural Characterization, and Reactivity of the Tilted Bis(arene) Metal Complexes $[(C_6H_5)_2Si(\eta^6-C_6H_5)_2]M$ ($M = V, Cr$)[†]

Christoph Elschenbroich,* James Hurley, Bernhard Metz, Werner Massa, and Gerhard Baum

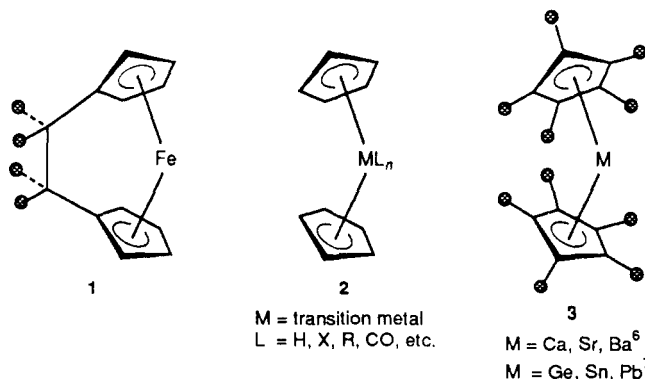
Fachbereich Chemie der Philipps-Universität, D-3550 Marburg, FRG

Received May 1, 1989

By means of lithiation and subsequent reaction with triphenylchlorosilane and diphenyldichlorosilane, respectively, the complexes bis((triphenylsilyl)- η^6 -benzene) M (**6**, $M = Cr$; **8**, $M = V$) as well as (1-6:1'-6'- η -tetraphenylsilane) M (**5**, $M = Cr$; **7**, $M = V$) were prepared and characterized by 1H and ^{13}C NMR (**5**, **6**) and EPR spectroscopies (**6**, **7**, **8**) and by cyclic voltammetry (**6**-**8**). **5** was subjected to X-ray crystallographic analysis; the complex crystallizes in the monoclinic space group $P2_1/n$ with $a = 764.7$ (3) pm, $b = 1854.5$ (8) pm, $c = 1261.8$ (5) pm, $\beta = 93.60$ (3)°, and $Z = 4$. The most pertinent features of the molecular structure of **5** are the tilting angle of the sandwich axis (165.6°), the bending of the ipso C-Si bond out of the η^6 -arene plane by 40.8°, and the small angle C(η -arene)-Si-C(η -arene) of 95.9°. Judging from the C-C bond lengths and ^{13}C chemical shifts, the ipso C atoms of the coordinated arenes are in a hybridization state between sp^2 and sp^3 . The deviation of the two η -arenes from a parallel disposition exerts a significant influence on ring proton chemical shifts, equivalent protons having the smallest interannular separations being shifted farthest upfield. For the paramagnetic vanadium analogues, EPR measurements further show that tilting is accompanied by an increase in metal \rightarrow ligand spin delocalization. The single-atom-bridged tilted complexes **5** and **7** are labile in solution. Whereas for the chromium species **5** protodesilylation to yield unsubstituted bis(benzene)chromium (**9**) dominates, the vanadium species **7** undergoes metal-ligand cleavage. Tilting exerts only a minor influence on the redox potential since $E_{1/2}$ for the couple $7^{0/-}$ lies approximately halfway between the $E_{1/2}$ values for 1- Ph_3Si - and 1,1'-(Ph_3Si)₂-substituted bis(benzene)-vanadium.

The chemistry of bis(η^5 -cyclopentadienyl) transition-metal complexes abounds with species displaying tilted sandwich units, bending being effected either by short interannular bridges as in [n]ferrocenophanes **1** ($n = 2, 2^3$) or by the presence of ancillary ligands as in ternary complexes of the type Cp_2ML_n (**2**).^{4,5}

In the case of certain main-group central metals, tilted complexes **3** arise even in the absence of the constraints mentioned above. Evidence for tilted bis(η^6 -arene)metal units is scarce. Apart from the weakly bonded adducts between group 13 metal halides and arenes⁸ and the complex (5,12:6,11-dimethano-5,5a,6,11,11a,12-hexahydro- η^{12} -tetracene)chromium,⁹ where the ligand represents a [3.3]orthocyclophane derivative, the compounds [(arene)₂WH]PF₆,¹⁰ [(C₆H₅Me)₂MPMe₃] ($M = Zr, Hf$),^{11a} [(C₆H₅Me)₂NbX] ($X = Me, Ph, Br, I$),^{11b} and



[(C₆H₅Me)₂M(SnMe₃)₂] ($M = Zr, Hf$)¹² appear to be the only examples in this class. Our interest in tilted bis(arene)

[†] Dedicated to Professor Dirk Reinen on the occasion of his 60th birthday.

(1) Part 33: Elschenbroich, C.; Schneider, J.; Massa, W.; Baum, G.; Mellinghoff, H. *J. Organomet. Chem.* 1988, 355, 163.

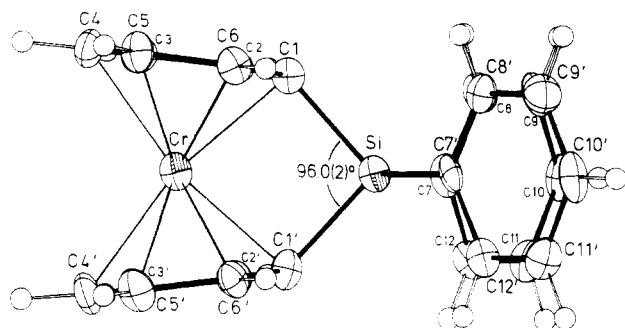
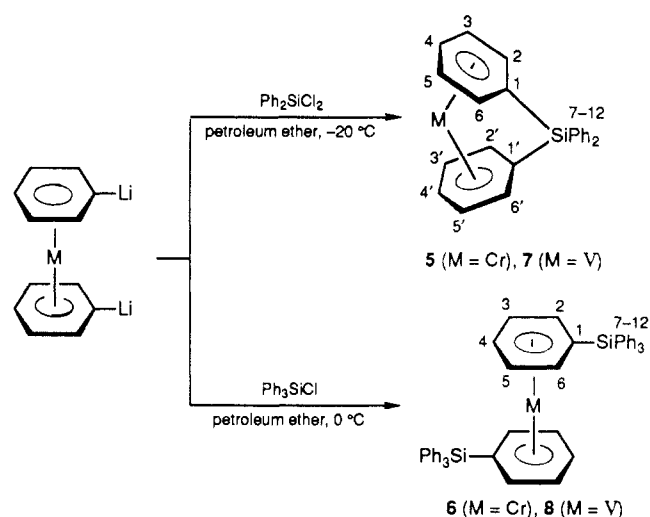


Figure 1. ORTEP³³ drawing of the structure of the complex $[(C_6H_5)_2Si(\eta^6-C_6H_5)_2]Cr$ (5) at the 50% probability level, also indicating the numbering scheme.

Scheme I



transition-metal complexes derives from the influence tilting may exert on electronic structure and reactivity. In this paper we report on the synthesis of the first bis(arene)metal complexes featuring one-atom interannular bridges.¹³ In contrast, for the class of metallocenes species

Table I. Experimental Data for the Crystal Structure Determination of the Complex 5

Crystal Data	
formula	$C_{24}H_{20}SiCr$
cryst dimens	approx $0.78 \times 0.27 \times 0.24$ mm ³
abs	$\mu = 16.2$ cm ⁻¹ , ψ -scan cor
space group	$P2_1/n$ ($Z = 4$)
lattice const (Cu K α)	$a = 764.7$ (3) pm $b = 1854.5$ (8) pm $c = 1261.8$ (5) pm $\beta = 93.60$ (3) ^o
temp	135 K
density	$d_c = 1.938$ g cm ⁻³
Data Collection	
diffractometer	4-circle, CAD4 (Enraf-Nonius)
radiation	Cu K α , graphite monochromator
scan type	ω -scan
scan width	$(0.8 + 0.14 \tan \theta)^\circ$ and 25% on the left and right side of a rfln for bkgd deternn
measuring range	$2^\circ < \theta < 50^\circ$ ($\pm h, \pm k, \pm l$)
no. of rflns	6884, 1737 unique ($>3\sigma(F_o)$)
Computing	
struct soln	Patterson methods (SHELXS-86 ^a)
refinement	full matrix, $\sum w\Delta^2$ minimized (SHELX76 ^b), $w = 1/\sigma^2(F_o)$
extinctn param	$\epsilon = 1.5$ (3) $\times 10^{-6}$ (after refinement)
R values	$R = 0.046$, $R_g = R_w = 0.042$

^a Sheldrick, G. M. *SHELXS-86, Program for Crystal Structure Solution*; University of Göttingen: Göttingen, FRG, 1986.
^b Sheldrick, G. M. *SHELX76, Program for Crystal Structure Determination*; Cambridge University: Cambridge, U.K., 1976.

Table II. Fractional Atomic Coordinates and Equivalent Isotropic Temperature Factors for the Non-Hydrogen Atoms in 5 with Estimated Standard Deviations in Parentheses^a

atom	x	y	z	U_{eq}/U_{iso}
Cr	0.0231 (1)	0.37539 (4)	0.83015 (5)	0.0262 (3)
Si	-0.1510 (2)	0.30183 (6)	0.9908 (1)	0.0245 (4)
C1	0.0831 (5)	0.3316 (2)	0.9829 (3)	0.023 (2)
C2	0.1766 (5)	0.2935 (2)	0.9066 (3)	0.024 (2)
C3	0.2803 (6)	0.3282 (2)	0.8350 (3)	0.027 (2)
C4	0.2979 (6)	0.4036 (2)	0.8380 (3)	0.027 (2)
C5	0.2149 (5)	0.4426 (2)	0.9139 (3)	0.026 (2)
C6	0.1093 (5)	0.4081 (2)	0.9851 (3)	0.025 (2)
C7	-0.1699 (6)	0.2015 (2)	0.9974 (3)	0.025 (2)
C8	-0.0505 (6)	0.1603 (3)	1.0602 (3)	0.027 (2)
C9	-0.0680 (6)	0.0875 (3)	1.0688 (3)	0.029 (2)
C10	-0.2050 (6)	0.0523 (2)	1.0149 (3)	0.029 (2)
C11	-0.3262 (6)	0.0911 (3)	0.9526 (3)	0.029 (2)
C12	-0.3090 (6)	0.1648 (2)	0.9437 (3)	0.027 (2)
C1'	-0.2301 (6)	0.3368 (2)	0.8562 (3)	0.023 (2)
C2'	-0.1625 (5)	0.2991 (2)	0.7694 (3)	0.026 (2)
C3'	-0.0970 (6)	0.3349 (3)	0.6825 (3)	0.029 (2)
C4'	-0.0967 (6)	0.4099 (3)	0.6785 (3)	0.031 (2)
C5'	-0.1681 (6)	0.4491 (2)	0.7606 (3)	0.030 (2)
C6'	-0.2348 (5)	0.4132 (2)	0.8469 (3)	0.024 (2)
C7'	-0.2605 (6)	0.3455 (2)	1.1024 (3)	0.022 (2)
C8'	-0.1720 (6)	0.3589 (2)	1.996 (3)	0.027 (2)
C9'	-0.2582 (6)	0.3865 (2)	1.2840 (3)	0.034 (2)
C10'	-0.4342 (6)	0.4014 (2)	1.2729 (3)	0.031 (2)
C11'	-0.5236 (6)	0.3884 (2)	1.1773 (3)	0.031 (2)
C12'	-0.4376 (6)	0.3606 (2)	1.0934 (3)	0.026 (2)

$$^a U_{eq} = (\sum_i \sum_j U_{ij} a_i^* a_j^* a_i a_j) / 3 \text{ (\AA}^2\text{)}.$$

with one-atom inter-ring bridges ([1]ferrocenophanes) have already been prepared in considerable number, P, As, Si,

(13) Whereas the nomenclature of metallocenophanes is based on the name of the parent bis(cyclopentadienyl)metal complex¹⁴ (example: 1 = [2]ferrocenophane), we regard interannularly bridged bis(arene)metal complexes as derivatives of the parent cyclophane, the latter usually also existing as a free ligand (example: (octamethyltetrasilane- η^{12} -[2.2]paracyclophane)chromium (4)¹⁵).

- (2) (a) Laing, M. B.; Trueblood, K. N. *Acta Crystallogr.* **1965**, *19*, 373.
(b) Lentzner, H. L.; Watts, W. E. *J. Chem. Soc., Chem. Commun.* **1970**, 26.
(c) Lentzner, H. L.; Watts, W. E. *Tetrahedron* **1971**, *27*, 4343.
(d) Yasufuku, K.; Aoki, K.; Yamazaki, H. *Inorg. Chem.* **1977**, *16*, 624.
(3) (a) Stoeckli-Evans, H.; Osborne, A. G.; Whitely, R. H. *Helv. Chim. Acta* **1976**, *59*, 2402.
(b) Seyferth, D.; Withers, H. P., Jr. *Organometallics* **1982**, *1*, 1275.
(c) Withers, H. P., Jr.; Seyferth, D.; Fellman, J. D.; Garron, P. E. *Organometallics* **1982**, *1*, 1283.
(d) Wrighton, M. S.; Palazzotto, M. C.; Bocarsly, A. B.; Bolts, J. M.; Fischer, A. B.; Nadjio, L. *J. Am. Chem. Soc.* **1978**, *100*, 7264.
Fischer, A. B.; Kinney, J. B.; Staley, R. H.; Wrighton, M. S. *J. Am. Chem. Soc.* **1979**, *101*, 6501.
Fischer, A. B.; Bruce, J. A.; McKay, D. R.; Maciel, G. E.; Wrighton, M. S. *Inorg. Chem.* **1982**, *21*, 1766.
Osborne, A. G.; Whiteley, R. H.; Meads, R. E. *J. Organomet. Chem.* **1980**, *193*, 345.
(e) Butler, R. O.; Culllan, W. R.; Einstein, F. W. B.; Rettig, S. J.; Willis, A. J. *Organometallics* **1983**, *2*, 128.
(4) Green, M. L. H. *Pure Appl. Chem.* **1972**, *30*, 373.
(5) For leading references, see: Lauher, J. W.; Hoffmann, R. *J. Am. Chem. Soc.* **1976**, *98*, 1729.
(6) Anderson, R. A.; Blom, R.; Burns, C. J.; Volden, H. V. *J. Chem. Soc., Chem. Commun.* **1987**, 768.
(7) Jutzi, P. *Adv. Organomet. Chem.* **1986**, *26*, 217.
(8) Schmidbaur, H. *Angew. Chem., Int. Ed. Engl.* **1985**, *24*, 893; **1987**, *26*, 338.
(9) Elschenbroich, C.; Schneider, J.; Prinzbach, H.; Fessner, W.-D. *Organometallics* **1986**, *5*, 2091.
(10) Cloke, F. G. N.; Green, M. L. H.; Morris, G. E. *J. Chem. Soc., Chem. Commun.* **1978**, 72.
(11) (a) Cloke, F. G. N.; Green, M. L. H. *J. Chem. Soc., Chem. Commun.* **1979**, 127.
(b) Green, M. L. H.; O'Hare, D.; Watkin, J. D. *J. Chem. Soc., Chem. Commun.* **1989**, 698.
(12) Cloke, F. G. N.; Cox, P. K.; Green, M. L. H.; Bashkin, J.; Prout, K. *J. Chem. Soc., Chem. Commun.* **1981**, 117.

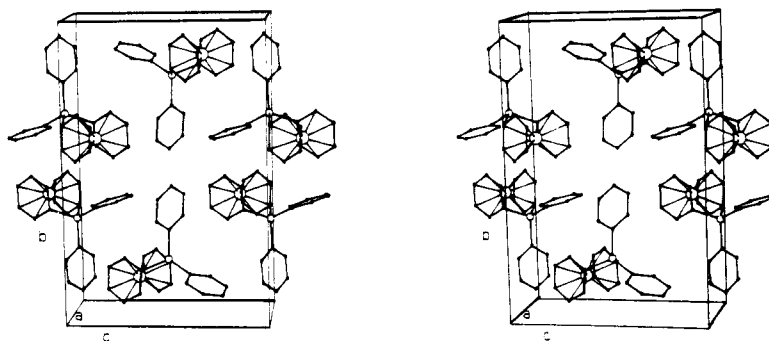
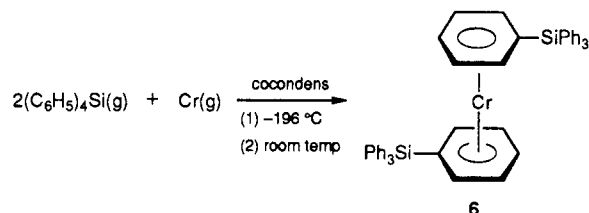


Figure 2. Stereoview of **5** showing the packing in the unit cell and Ge serving as bridging atoms.³

Results and Discussion

Initial attempts to prepare $[(C_6H_5)_2Si(\eta^6-C_6H_5)_2]Cr$ (**5**) by cocondensation of tetraphenylsilane with chromium atoms were unsuccessful. Under these conditions the main product is the unbridged species $[(C_6H_5)_3Si-\eta^6-C_6H_5]_2Cr$ (**6**). Rather, **5** and its vanadium analogue **7** can be pre-



pared by coupling the respective 1,1'-dilithiated bis(arene)metal complexes with diphenyldichlorosilane. The corresponding unbridged bis(triphenylsilyl) derivatives **6** and **8** are obtained from metathetical reactions with triphenylchlorosilane (Scheme I).¹⁶ The bridged species (1-6:1'-6'- η -tetraphenylsilane)chromium (**5**) and -vanadium (**7**) form maroon and black air-sensitive crystals, respectively, of moderate thermal stability. However, in the presence of protic impurities the complexes **5** and **7** readily undergo cleavage of the interannular $-Ph_2Si-$ bridge, **5** being more prone than **7** to this degradation process.

Molecular Geometry of $[(C_6H_5)_2Si(\eta^6-C_6H_5)_2]Cr$. The molecular structure of **5** as determined by an X-ray structural analysis is shown in Figures 1 and 2; bond lengths and bond angles are listed in Tables III and IV. Upon coordination, two of the phenyl groups of the tetraphenylsilane ligand adopt a nearly parallel disposition reminiscent of the sandwich structure of bis(benzene)chromium (**9**). However, the bridging $SiPh_2$ linkage effects a tilting of the planar, coordinated phenyl groups by 14.4° . Therefore, large differences in the interannular distances between symmetry-equivalent carbon atoms accrue that show the gradation 290 (ipso), 315 (ortho), 353 (meta), and 371 (para) pm. Thus, whereas the mean inter-ring distance (332 pm) is only slightly enlarged, compared to that of undistorted bis(η^6 -benzene)chromium (**9**, 322 pm¹⁷), sizable compression and elongation is effected for the ipso and the

Table III. Bond Lengths (Å) and Selected Bond Angles (deg) in 5

Cr...Si	2.842 (2)	Cr-C1	2.115 (4)
Cr-C2	2.116 (4)	Cr-C3	2.150 (4)
Cr-C4	2.162 (4)	Cr-C5	2.152 (4)
Cr-C6	2.113 (4)	Cr-C1'	2.109 (4)
Cr-C2'	2.114 (4)	Cr-C3'	2.159 (4)
Cr-C4'	2.166 (4)	Cr-C5'	2.149 (4)
Cr-C6'	2.116 (4)	Si-C1	1.882 (4)
Si-C1'	1.882 (4)	Si-C7	1.870 (5)
Si-C7'	1.868 (4)	C1-C2	1.422 (6)
C1-C6	1.433 (6)	C2-C3	1.397 (6)
C3-C4	1.405 (6)	C4-C5	1.386 (6)
C5-C6	1.400 (6)	C7-C8	1.397 (6)
C7-C12	1.401 (6)	C8-C9	1.363 (7)
C9-C10	1.377 (7)	C10-C11	1.380 (6)
C11-C12	1.379 (7)	C1'-C2'	1.424 (6)
C1'-C6'	1.423 (6)	C2'-C3'	1.401 (6)
C3'-C4'	1.392 (7)	C4'-C5'	1.403 (6)
C5'-C6'	1.400 (6)	C7'-C8'	1.385 (6)
C7'-C12'	1.380 (6)	C8'-C9'	1.385 (6)
C9'-C10'	1.372 (7)	C10'-C11'	1.371 (6)
C11'-C12'	1.381 (6)		
C1-Si-C1'	96.0 (2)	C1-Si-C7	111.8 (2)
C1-Si-C7'	112.7 (2)	C1'-Si-C7	111.3 (2)
C1'-Si-C7'	113.4 (2)	C7-Si-C7'	110.9 (2)
Si-C1-C2	114.2 (3)	Si-C1'-C2'	114.4 (3)
Si-C1-C6	114.9 (3)	Si-C1'-C6'	115.0 (3)
C2-C1-C6	115.4 (4)	C2'-C1'-C6'	115.8 (4)
C1-C2-C3	122.6 (4)	C1'-C2'-C3'	122.3 (4)
C2-C3-C4	119.9 (4)	C2'-C3'-C4'	120.3 (4)
C3-C4-C5	119.4 (4)	C3'-C4'-C5'	119.3 (4)
C4-C5-C6	120.8 (4)	C4'-C5'-C6'	120.4 (4)
C1-C6-C5	121.7 (4)	C1'-C6'-C5'	121.9 (4)
Si-C7-C8	121.3 (3)	Si-C7'-C8'	121.9 (3)
Si-C7-C12	121.3 (3)	Si-C7'-C12'	120.6 (3)
C8-C7-C12	117.4 (4)	C8'-C7'-C12'	117.3 (4)
C7-C8-C9	121.5 (4)	C7'-C8'-C9'	121.2 (4)
C8-C9-C10	120.4 (4)	C8'-C9'-C10'	120.5 (4)
C9-C10-C11	119.8 (4)	C9'-C10'-C11'	119.1 (4)
C10-C11-C12	120.0 (4)	C10'-C11'-C12'	120.4 (4)
C7-C12-C11	120.9 (4)	C7'-C12'-C11'	121.6 (4)

para carbon atom pairs. Slippage is very small in that the perpendicular projections of the chromium atom on the ring least-squares planes deviate from the ring centers by only 5 pm. Consequently, the chromium-carbon distances are rather similar ($d(Cr-C) = 211, 212, 215, 216$ pm in **5**) and comparable to those in bis(benzene)chromium ($d(Cr-C) = 213$ pm¹⁷).

Whereas the bond angle $C(7)-Si-C(7')$ (110.9°) deviates only marginally from the tetrahedral angle, the corresponding $C(1)-Si-C(1')$ bond angle is reduced to 95.9° . The bond axes $Si-C(1)$ and $Si-C(1')$ are bent out of the mean plane of the η^6 -arenes by 40.8° . Marked bond angle distortions are also observed for the segments $C(2)-C(1)-C(6)$ and $C(2')-C(1')-C(6')$ (115.4°), respectively. The $Si-C$ bond distances are equivalent within experimental

(14) Mueller-Westerhoff, U. T. *Angew. Chem., Int. Ed. Engl.* **1986**, *25*, 702.

(15) Elschenbroich, C.; Hurley, J.; Massa, W.; Baum, G. *Angew. Chem., Int. Ed. Engl.* **1988**, *27*, 684.

(16) By the same procedure, derivatives containing $-SiCl_2-$ and $-SiMe_2-$ bridges are accessible: Elschenbroich, C.; Hurley, J. To be submitted for publication.

(17) Haaland, A. *Acta Chem. Scand.* **1965**, *19*, 41. Keulen, E.; Jellinek, F. *J. Organomet. Chem.* **1965**, *5*, 490.

(18) Compare the protodesilylation of silylferrocenes: Kumada, M.; Kondo, T.; Mimura, K.; Yamamoto, K.; Ishikawa, M. *J. Organomet. Chem.* **1972**, *43*, 307.

Table IV. Distances (pm) from "Best Planes" through the Atoms Labeled by an Asterisk and Selected Interplanar Angles (deg)

Plane 1							
C1*	C2*	C3*	C4*	C5*	C6*	Cr	Si
-1.8 (12)	1.4 (12)	0.2 (11)	-1.5 (11)	1.0 (11)	0.6 (11)	-160.5 (9)	-125 (1)
Plane 2							
C1'*	C2'*	C3'*	C4'*	C5'*	C6'*	Cr	Si
2.1 (11)	-0.9 (11)	-0.9 (10)	1.6 (9)	-0.4 (9)	-1.4 (10)	160.6 (10)	125 (1)
Plane 3							
C7*	C8*	C9*	C10*	C11*	C12*	Si	
-0.2 (21)	0.0 (22)	0.2 (24)	-0.4 (24)	0.2 (23)	0.0 (22)	7.4 (20)	
Plane 4							
C7'*	C8'*	C9'*	C10'*	C11'*	C12'*	Si	
-0.1 (19)	-0.1 (20)	0.2 (21)	-0.1 (21)	-0.1 (20)	0.2 (18)	12.6 (17)	
Interplanar Angles							
planes 1-2		14.4 (2)		planes 3-4		104.6 (2)	
Bond/Plane Angle							
Si-C1/plane 1		139.1 (2)		Si-C7/plane 3		177.7 (2)	
Si-C1'/plane 2		139.4 (2)		Si-C7'/plane 4		176.1 (2)	

Table V. ^1H and ^{13}C NMR Spectral Data for the Ligand Ph_3Si (11) and for the Complexes $(\text{Ph}_3\text{Si}-\eta^6\text{-C}_6\text{H}_5)_2\text{Cr}$ (6) and $[\text{Ph}_2\text{Si}(\eta^6\text{-C}_6\text{H}_5)_2]\text{Cr}$ (5)

compd	<i>i</i>	$\delta(^1\text{H}_i)^a$	$\Delta\delta(^1\text{H}_i)^b$	<i>i,j</i>	$J(^1\text{H}_i, ^1\text{H}_j)^c$	<i>i</i>	$\delta(^{13}\text{C}_i)^a$	$\Delta\delta(^{13}\text{C}_i)^b$	<i>i,j</i>	$J(^{13}\text{C}_i, ^1\text{H}_j)^c$
11	2,6	7.66		2,3	7.7	1	134.8			
				2,4	1.8	2,6	128.3		2,2	158.5
	3-5	7.17-7.26		m		3,5	136.9		3,3	158.5
						4	129.9		4,4	159.4
6						1	73.2	-61.6		
	2,6	4.48	-3.18	br s		2,6	81.4	-46.9	2,2	
						3,5	77.4	-59.5	3,3	
						4	74.3	-55.6	4,4	
	3-5	4.30	-2.92	br s		7	135.7	0.9		
	8,12	7.77	0.11		8,9	7.6	8,12	136.8	8.5	8,8
				8,10	1.8	9,11	128.1	-8.8	9,9	158.4
	9-11	7.16-7.21	~0	m		10	129.8	-0.1	10,10	
						1	37.7	-97.1		
5	2,6	4.16	-3.50	2,3	5.2	2,6	77.2	-51.1	2,2	168.8
	3,5	4.44	-2.78	2,3; 3,4	5.6	3,5	83.1	-53.8	3,3	166.7
	4	4.70	-2.52	3,4	5.4	4	79.7	-50.2	4,4	169.0
						7	134.5	-0.3		
	8,12	8.06	0.40	8,9	7.6	8,12	134.6	6.3		158.3
				8,10	1.8					
	9-11	7.20-7.27	0.05			9,11	128.9	-8.0		158.5
						10	130.2	0.3		

^aChemical shift (ppm) referenced to TMS, measured in C_6D_6 . ^bCoordination shift $\delta(\text{complex}) - \delta(\text{ligand})$. ^cCoupling constant (Hz).

error, however. Within the $\eta^6\text{-C}_6\text{H}_5$ rings significant differences in the C-C bond lengths are encountered, the bonds radiating from the ipso carbon atoms C(1) and C(1') (average 142.5 pm) being longer than the remaining C-C bonds in the coordinated arenes (average 138.9 pm) and all C-C bonds in the free arenes (average 138.1 pm). This finding, together with the bond angles around C(1) and C(1'), reflects a carbon hybridization intermediate between sp^2 and sp^3 , which (inter alia) manifests itself in the position of the ^{13}C NMR signal.

Nuclear Magnetic Resonance. The coordination shift $\Delta\delta(^1\text{H})$ in the proton magnetic resonance spectra of ($\eta^6\text{-arene}$)metal complexes shows a pronounced dependence on the geometric disposition of the respective protons relative to the ring center.^{9,19} In Figure 3 the ^1H NMR spectra of tilted 5, untilted 6, and the free ligand tetraphenylsilane (11) are displayed; the relevant data are collected in Table V. Since in both complexes 5 and 6

the $\eta^6\text{-arenes}$ are substituted by a triphenylsilyl group, the differences in shielding may be attributed to tilting of the sandwich structure, rather than to differing electronic effects exerted by the substituents. Inspection of the shift range $5 > \delta(^1\text{H}) > 4$ ppm reveals that the changes in shielding, caused by the introduction of the SiPh_2 bridge, correlate linearly with the variation in interannular proton distance. This relationship is illustrated in Figure 5. Here the deviations of the chemical shifts $\delta(^1\text{H}, \eta\text{-arene})$ for the ortho, meta, and para protons of 5 from the respective values in nontilted 6 are plotted against the deviations of the interannular proton distances in 5 from those in 6. For 6 the inter-ring distance (322 pm) of bis(benzene)chromium is adopted since the introduction of two Ph_3Si substituents is not expected to significantly modify the former. The dependence of proton shielding in 5 on the inter-ring distance illustrates a phenomenon widely observed in cyclophanes, which consists of high-field shifts as a result of face-to-face stacking of arenes, one ring being positioned in the shielding region of the other ring.²⁰ Small coordination shifts are also observed for the ortho

(19) Elschenbroich, C.; Spangenberg, B.; Mellinghoff, H. *Chem. Ber.* 1984, 117, 3165. Elschenbroich, C.; Koch, J.; Schneider, H.; Spangenberg, B.; Schiess, P. *J. Organomet. Chem.* 1986, 317, 41. Elschenbroich, C.; Schneider, J.; Mellinghoff, H. *J. Organomet. Chem.* 1987, 333, 37. McGlinchey, M. J.; Burns, R. C.; Hofer, R.; Top, S.; Jaouen, E. *Organometallics* 1986, 5, 104.

(20) For leading references, see: Boekelheide, V. *Top. Curr. Chem.* 1983, 113, 87.

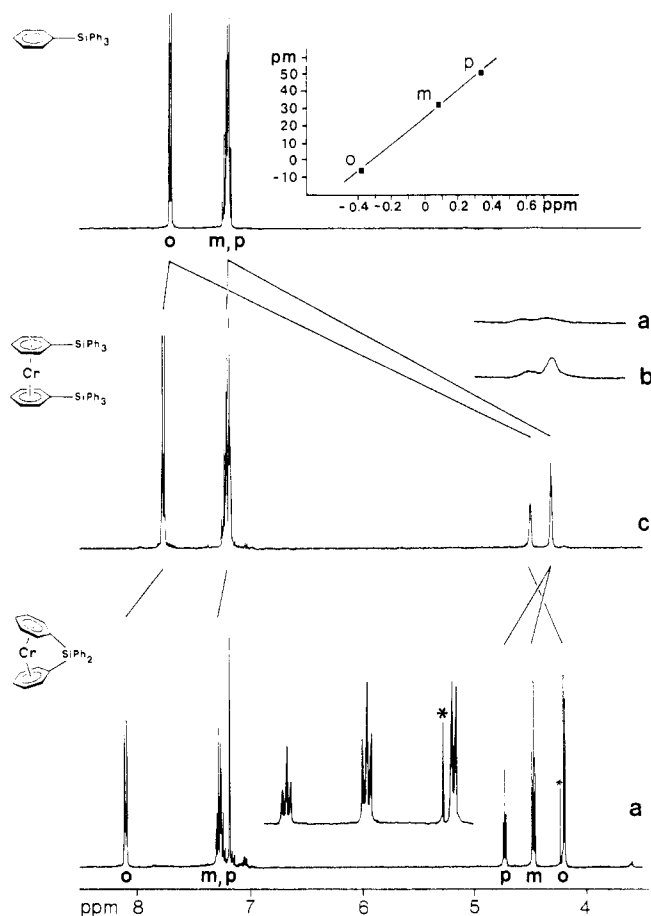


Figure 3. ^1H NMR spectra (300 MHz) of Ph_4Si (11), $(\text{Ph}_3\text{Si}\eta^6\text{-C}_6\text{H}_5)_2\text{Cr}$ (6), and $[\text{Ph}_2\text{Si}(\eta^6\text{-C}_6\text{H}_5)_2]\text{Cr}$ (5) in C_6D_6 at room temperature: (a) initial spectrum; (b) spectrum after 5-h storage at 70 °C; (c) spectrum after 2-day storage at 70 °C. The inset gives a plot depicting the effect of tilting the arene-metal-arene axis in 5 on magnetic shielding of the arene protons: (ordinate) deviation of the interannular proton distance in 5 from that in the parent complex 9; (abscissa) deviation of $\delta(^1\text{H},5)$ from the respective chemical shift $\delta(^1\text{H},9)$. The signal marked with an asterisk stems from $(\eta^6\text{-C}_6\text{H}_5)_2\text{Cr}$ (9).

protons of the noncoordinated phenyl rings in 5. This may be explained by the fact that the conversion of free tetraphenylsilane into the complex 5 places the ortho protons of the uncoordinated rings in the deshielding region of the coordinated arenes. Tilting also exerts a dramatic effect on the ^{13}C NMR spectrum in that the ipso carbon resonance experiences a 35.5 ppm upfield shift upon proceeding from 6 to 5. This unquestionably is a consequence of bond angle distortion about C(1), resulting in a change in carbon hybridization from sp^2 toward sp^3 . The marked lengthening of the C-C bonds radiating from C(1) points in the same direction. Similar unusually strong shielding for carbon atoms that are part of conjugated systems has been observed for single heteroatom bridged ferrocenophanes.^{3a,d}

Protodesilylation. The lability of C-Si bonds in η^6 -silylarenes toward solvolytic cleavage is well established.²¹ In the case of 5, the siloxane 10 is formed as inferred from ^1H NMR and mass spectrometric analysis. 10 is further desilylated to yield bis(benzene)chromium (Scheme II). Interestingly, extended exposure to LiOEt in DME leaves 5 unaffected, whereas in the medium THF/5% H_2O cleavage of the bridge occurs instantaneously. Therefore,

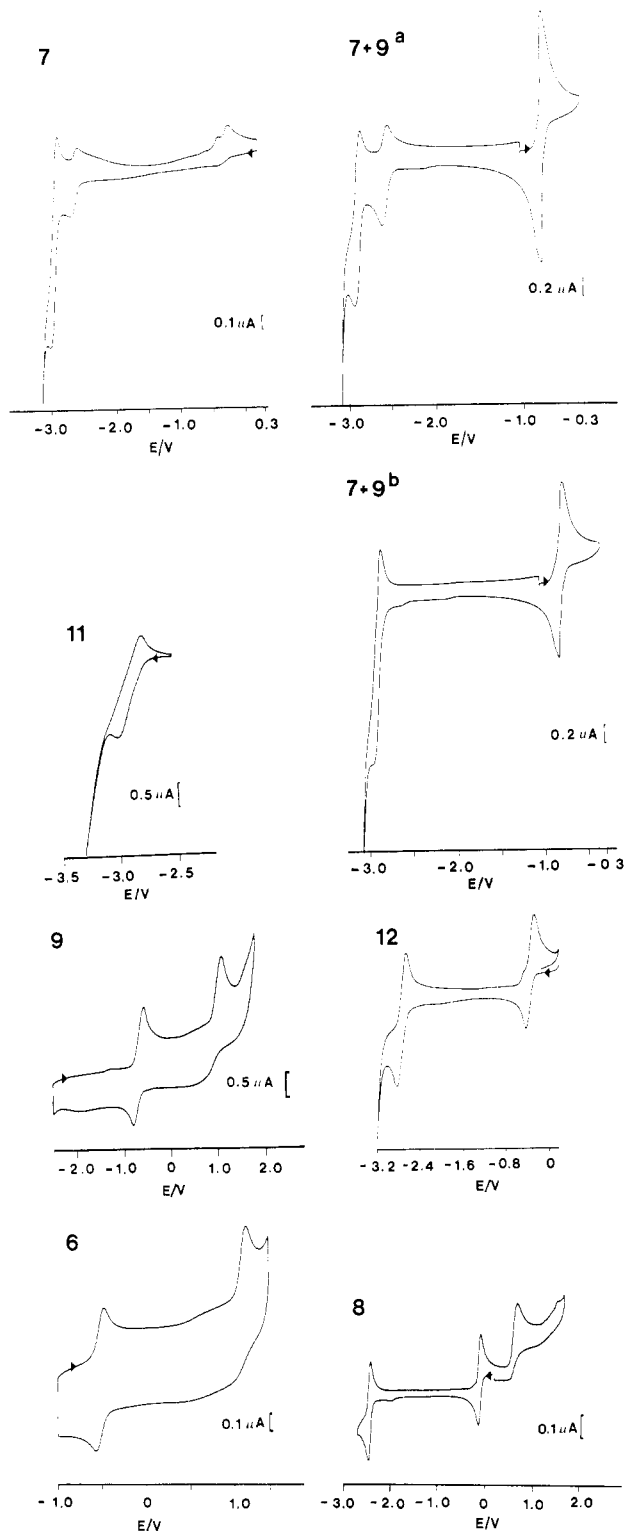


Figure 4. Cyclic voltammograms for the chromium complexes 9 and 6, the vanadium complexes 12, 8, and 7, and the ligand 11 in DME/ Bu_4NClO_4 : (a) after 1 h at 20 °C; (b) After 12 h at -60 °C. Conditions and electrochemical parameters are collected in Table IV.

cleavage of the C-Si bond in 5 most likely is initiated by electrophilic attack of H^+ at the ipso carbon atom¹⁸ (Scheme II).

The exceedingly high vulnerability of the $\text{C}_{\text{arene}}\text{-Si}$ bond in 5 may be rationalized on the basis of its structural features and the position of the ^{13}C NMR signal for C_1 . In 5, the geometry around C_1 approaches that required for the Wheland-type transition state of electrophilic aromatic substitution. Furthermore, the energy of the cationic

(21) (a) Elschenbroich, C. *J. Organomet. Chem.* 1970, 22, 677. (b) Elschenbroich, C.; Koch, J.; Kroker, J.; Wünsch, M.; Massa, W.; Baum, G.; Stork, G. *Chem. Ber.* 1988, 121, 1983.

Table VI. Electrochemical Data^a for the Complexes 12, 8, 7, 9, and 6 and for the Ligands Ph₄Si (11) and Ph-Ph (13)

compd	couple	E_{pc} , V	E_{pa} , V	$E_{1/2}$, V ^b	ΔE_p , mV	i_{pa}/i_{pc}	ν , mV s ⁻¹	T , °C
12	0/-			-2.67 (r)			100	-60
	0/+			-0.36 (r)				
8	0/-	-2.52	-2.43	-2.48 (q)	90	0.85	100	-60
	0/+	-0.195	-0.125	-0.16 (r)	70	1.1	20	
7	0/-	-2.584	-2.494	-2.54 (q)	91	0.66	200	-60
	0/+		-0.164	i			100	
9	0/- ^d							+25
	0/+	-0.755	-0.615	-0.685 (r)	140	1.03	100	
6	0/-	-2.875	-2.750	-2.813 (q)	125	<i>e</i>		-50
	0/+	-0.590	-0.510	-0.550 (r)	80	0.95	50	
11	0/-	-2.92	-2.78	-2.85 (q)	140 ^c	0.92	20	-60
13	0/-	-2.70	-2.49	-2.60 (q)	210 ^c	0.92	100	-26

^a In 1,2-dimethoxyethane/0.1 M tetraethylammonium perchlorate at a glassy-carbon electrode versus the saturated calomel electrode. ^b Legend: r, reversible, q, quasi-reversible; i, irreversible. ^c ΔE_p increases with increasing ν . ^d Not observable, $E_{1/2} < -3$ V. ^e Variable.

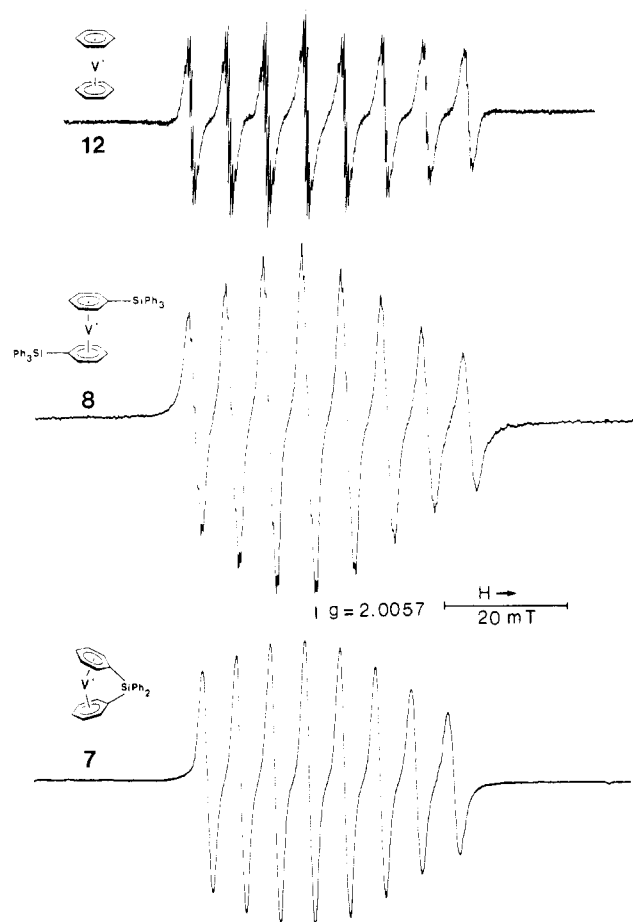
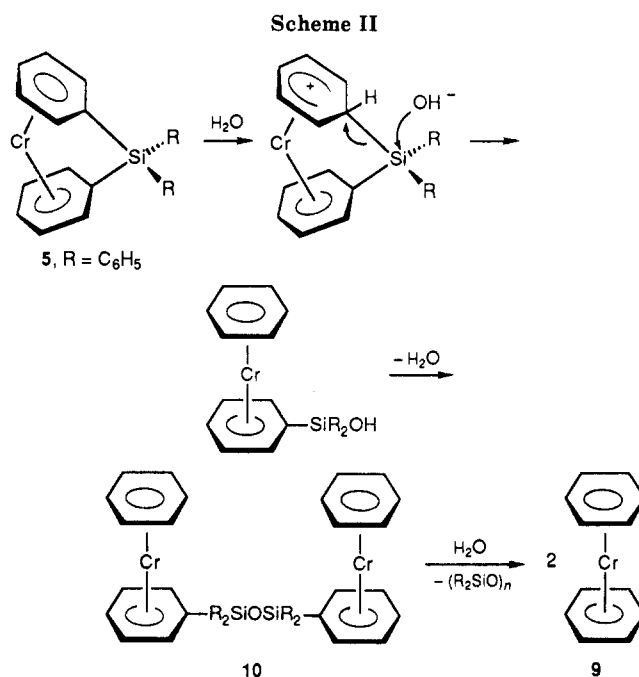


Figure 5. EPR spectra of the complexes 12, 8, and 7 in fluid solution (toluene, 30 °C).

transition state should be low since the formal positive charge in the η^5 -cyclohexenyl segment will be compensated by electron donation from the zerovalent central metal atom. In comparison to the case for the strained complex 5, in the unstrained species 6 the propensity toward protodesilylation is considerably attenuated. This is clearly apparent from the differing time spans required to obtain high-resolution ¹H NMR spectra in the η -arene region (Figure 3). Whereas in the case of 5 narrow-line ¹H NMR spectra are observed immediately after preparing the sample, for 6 an extended period of thermal treatment at +70 °C is necessary to ensure small line widths. Obviously, in the case of unstrained 6 both the neutral diamagnetic species and the radical cation 6⁺, adventitiously present,

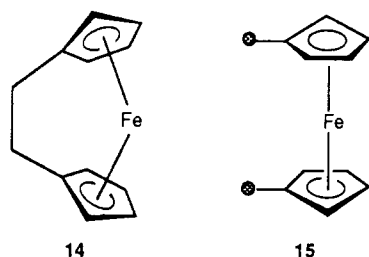


coexist for several hours at +70 °C, engaging in the self-exchange $6 + 6^+ = 6^+ + 6$ and thereby broadening the ¹H NMR lines.²² In the strained sila[1]chromocyclophane 5, on the other hand, the interannular bridge of the paramagnetic exchange partner 5⁺ is rapidly cleaved, leading to a nontilted bis(benzene)chromium(I) derivative that, owing to its modified structure, does not exhibit self-exchange with 5.

Cyclic Voltammetry. In Figure 4, representative cyclic voltammetric traces for the silylsubstituted complexes 6–8 are depicted together with those for the parent molecules bis(benzene)chromium (9), bis(benzene)vanadium (12), and the free ligand 11 for comparison. The exceedingly high sensitivity of 5 to cleavage of the $-\text{SiR}_2-$ bridge prevented collection of cyclic voltammetric data for this chromium species. The vanadium complex 7, however, proved amenable to electrochemical study. In all cases, apart from 7, the first step of electrochemical oxidation is reversible. As shown in Figure 4, additional irreversible oxidation steps are observable at more positive potentials. Whereas reduction is reversible for 12 only, 6–8 are reduced

(22) Elschenbroich, C.; Zenneck, U. *J. Organomet. Chem.* **1978**, *160*, 125.

quasi-reversibly. The reduction of **9** must occur beyond the limit of -2.9 V set by the medium.²³ Interestingly, the potential $E_{1/2}$ for the couple $12^{0/-}$ is found to be similar to that of biphenyl ($13^{0/-}$) as predicted previously from competition experiments.²⁴ As expected from their π -acceptor character, triphenylsilyl groups as peripheral substituents on η^6 -arenes stabilize the lower oxidation state of the respective bis(arene)metal complex. In the case of 1,1'-disubstitution the anodic shifts of $E_{1/2}$ amount to $+135$ mV ($9^{0/+}$ versus $6^{0/+}$), to $+200$ mV ($12^{0/+}$ versus $8^{0/+}$), and to $+190$ mV ($12^{0/-}$ versus $8^{0/-}$), respectively. If instead of 1,1'-disubstitution by Ph_3Si groups an interannular SiPh_2 group is present, the anodic shift is reduced to $+130$ mV ($12^{0/-}$ versus $7^{0/-}$). This shift reflects the aggregate effects of silyl substitution and bending of the sandwich structure.²⁵ In this context, it is worth mentioning that the influence of bending on the redox potential of ferrocene derivatives is also rather small.²⁶ Since electrochemical data in our standard medium dimethoxyethane/ Bu_4NClO_4 were missing, we prepared [2]ferrocenophane (**14**)²⁷ in



order to compare its redox potential with that of 1,1'-dimethylferrocene (**15**). The considerable tilting distortion in **14** (interplanar angle $\theta = 23.2^\circ$, $E_{1/2} = 0.453$ V) causes an anodic shift of only 56 mV (**15**: $\theta = 0^\circ$, $E_{1/2} = 0.397$ V).

This observation may be used to rationalize the potential observed for the couple $7^{0/-}$. Assuming additivity of the substituent effects on the redox potentials of sandwich complexes,²⁸ from the potentials $E_{1/2}(12^{0/-})$ and $E_{1/2}(8^{0/-})$ a value of $\Delta E_{1/2} = +95$ mV per SiPh_3 group may be derived. The anodic shift of $+130$ mV as one proceeds from $12^{0/-}$ to $7^{0/-}$ may then be roughly apportioned into contributions stemming from silyl substitution ($+95$ mV) and tilting ($+35$ mV). In this argument, we regard the tilted complex **7** as a singly silyl-substituted derivative of **12**. The cyclic voltammogram of **7**, in addition to a wave at -2.54 V, shows a wave at -2.86 V, which is assigned to the reduction of the free ligand tetraphenylsilane (**11**). The

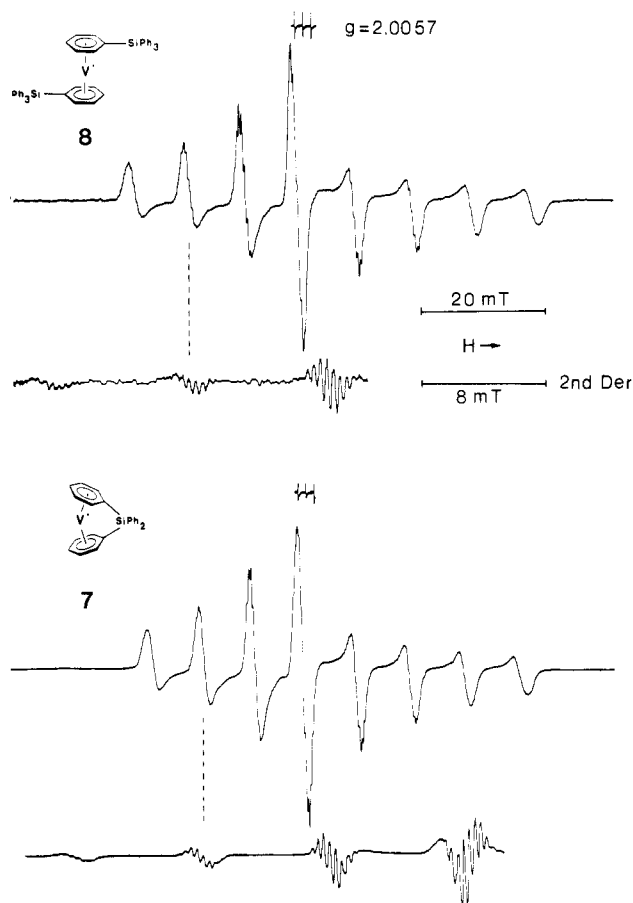


Figure 6. EPR spectra of the complexes **8** and **7** in rigid solution (toluene, -140°C).

Table VII. EPR Data for the Chromium(I) Complex Cations 9^+ and 6^+ and for the Vanadium(0) Complexes **12**, **8**, and **7** in Fluid (30°C) and Rigid (-140°C) Solution.

	$9^+{}^a$	$6^+{}^b$	12^c	8^d	7^d
$\langle g \rangle$	1.9867	1.9856	1.9860	1.9864	1.9866
g_{\perp}	1.979	1.9782	1.978	1.980	1.979
g_{\parallel}	2.002	2.001	2.001	1.999 ^e	2.002 ^e
$a(^1\text{H})$, mT	0.338	0.309	0.40	0.40	<i>f</i>
$a(^{53}\text{Cr}, ^{51}\text{V})$, mT	1.81	1.83	6.38	6.34	5.63
$A_{\perp}(^{53}\text{Cr}, ^{51}\text{V})$, mT	2.69	<i>f</i>	9.25	9.31	8.50
$A_{\parallel}(^{53}\text{Cr}, ^{51}\text{V})$, mT	0.05	<i>f</i>	0.64 ^e	0.40 ^e	0 ^e

^a Obtained via air oxidation of **9** in CHCl_3/DMF (1:1) (present work). See also: Prins, R.; Reinders, F. *J. Chem. Phys. Lett.* **1969**, *3*, 45. ^b In CHCl_3/DMF (1:1). ^c In toluene (present work). See also: Hauser, K. H. *Z. Naturforsch.* **1961**, *16A*, 1190. ^d In toluene. ^e Estimate according to $g_{\parallel} = 3\langle g \rangle - 2g_{\perp}$ and $A_{\parallel} = 3a - 2A_{\perp}$, respectively. ^f Not resolved.

(23) The chemical reduction of **9** requires forcing conditions; see: Elschenbroich, C.; Bilger, E.; Koch, J.; Weber, J. *J. Am. Chem. Soc.* **1984**, *106*, 4297.

(24) Elschenbroich, C.; Gerson, F. *J. Am. Chem. Soc.* **1975**, *97*, 3556.

(25) While it is true that structural parameters have been obtained by means of X-ray diffraction for the chromium complex **5** only, beyond any doubt the vanadium analogue **7** also features a tilted structure. In the latter case, bending of the sandwich axis may even be slightly more extensive since the interarene distance in the parent complex bis(η^6 -benzene)vanadium (**12**; 332 pm) exceeds that in the chromium congener **9** (322 pm). For a compilation of structural data of bis(arene)metals see: Muetterties, E. L.; Bleeke, J. R.; Wucherer, E. J.; Albright, T. A. *Chem. Rev.* **1982**, *82*, 499.

(26) (a) Fujita, E.; Gordon, B.; Hillman, M.; Nagy, A. G. *J. Organomet. Chem.* **1981**, *218*, 105. (b) El Sayed, A. M.; Seddon, E. A.; Seddon, K. R.; Shimran, A. A.; Tompkins, S. *J. Organomet. Chem.* **1988**, *347*, C25. (c) Vondrak, T. *Polyhedron* **1985**, *4*, 1271.

(27) Materikova, R. B.; Babin, V. N.; Solodovnikov, S. P.; Lyatifov, I. R.; Petrovsky, P. V.; Fedin, E. I. *Z. Naturforsch., B: Anorg. Chem., Org. Chem.* **1980**, *35B*, 1415.

(28) (a) Suskina, I. A.; Gribov, G. B.; Idrisova, R. A.; Danisovich, L. I.; Gubin, S. P. *Izv. Akad. Nauk SSSR, Ser. Khim.* **1971**, 425. (b) Sabatini, M. M.; Cesarotti, E. *Inorg. Chim. Acta* **1977**, *24*, L9. (c) Treichel, P. M.; Essenmacher, G. P.; Efner, H. F.; Klabunde, K. J. *Inorg. Chim. Acta* **1981**, *48*, 41.

latter wave grows at the expense of the former with time, the sum of the currents of these two waves remaining approximately constant (Figure 4). This change is accompanied by a gradual disappearance of the ESR spectrum of **7**. Obviously, in the medium $\text{DME}/\text{Bu}_4\text{NClO}_4$ **7** undergoes metal-ligand cleavage, for which at $T = -60^\circ\text{C}$ a half-life of about 4 h can be estimated. This behavior contrasts with that of the analogous chromium complex **5**, which under the same conditions is desilylated to yield bis(benzene)chromium. It therefore appears as if for the strained 17-valence-electron complex **7** associatively activated ligand displacement predominates, whereas in the case of the 18-valence-electron chromium congener **5**, bridge cleavage via electrophilic attack at the ipso carbon atom is the preferred mode of reaction.

Electron Spin Resonance. The extraordinarily high aptitude of **5** to undergo protodesilylation as yet has

prevented the generation and EPR identification of the radical cation 5^+ . Desilylation being attenuated at the neutral complex stage, an EPR study of **7** and related paramagnetic vanadium species is feasible, however. Representative EPR spectra, measured at +30 and -140 °C, are displayed in Figures 5 and 6, respectively. The corresponding magnetic parameters are collected in Table VII. In principle, tilting of an $(\eta^6\text{-arene})_2[\text{M}(\text{d}^5)]$ unit should result in a transformation of the \mathbf{g} tensor from axial (g_{\parallel}, g_{\perp}) to nonaxial (g_1, g_2, g_3) and in changes of central metal and ligand hyperfine coupling constants as a consequence of modified metal-ligand orbital overlap. Whereas the latter effect was observed for the $\text{Cr}(\text{d}^5)$ complex of a [3.3]orthocyclophane derivative,⁹ the effect of the tilting on g anisotropy was too small to be resolved. In the present case as well, loss of axial symmetry of the bis($\eta^6\text{-arene}$)vanadium unit does not perceptibly affect the \mathbf{g} tensor since, within the resolution attained, both **8** and **7** in rigid solution display spectra that are analyzed in terms of the two parameters g_{\parallel} and g_{\perp} . The marginal response of the \mathbf{g} tensor of orbitally nondegenerate bis($\eta^6\text{-arene}$)[metal(d^5)] complexes (ground state ${}^2A_{1g}$) to the tilting distortion contrasts with the behavior of ferrocenium ions (ground state ${}^2E_{2g}$), for which structural perturbations, due to concomitant raising of orbital degeneracy, profoundly modify the \mathbf{g} tensor.²⁹

Resolution of proton hyperfine structure for the derivatives **7** and **8** in fluid solution is inferior to that of the parent complex **12**. This is a consequence of the lower symmetry of **7** and **8**, which leads to several sets of magnetically inequivalent protons. The most pronounced change upon going from axial **8** to nonaxial **7** is the decrease (-12%) in the coupling constant $a(^1\text{H})$, which indicates that for the tilted complex **7** increased metal \rightarrow ligand spin delocalization prevails. This finding can be explained by resorting to a theoretical treatment of the bent bis(cyclopentadienyl) transition-metal unit Cp_2M in terms of changes in the molecular orbital compositions accompanying structural deformation.⁵ For the tilted metallocene the molecular orbital sequence $1a_1, b_2, 2a_1$ (=HOMO) has been derived, $1a_1$ and b_2 correlating with e_{2g} (M,L) and $2a_1$ with a_{1g} (M) of the untilted geometry. In the axially symmetric sandwich, the a_{1g} orbital is predominantly metal $3d_{z^2}$ in character, interaction with the aromatic ligands being negligible. In the bent sandwich, however, the HOMO $2a_1$ is allowed to mix with the sub-HOMO $1a_1$. Since the latter, being derived from e_{2g} , possesses a sizable ligand contribution, $2a_1$ will also acquire some ligand character. Thus, the singly occupied HOMO $2a_1$ provides for appreciable spin transfer to the ligands, leading to diminished spin population on the central metal as borne out in the spectrum of **7**.

A conspicuous EPR spectral change as a function of peripheral substitution is the dependence of the line widths on the nuclear spin quantum number $m_I(^{51}\text{V})$, which increases in the series $12 < 7 < 8$. Thus, the ratios of the square roots of the spectral amplitudes, $[A(m_I = +1/2)]^{1/2}/[A(m_I = -7/2)]^{1/2}$, which reflect the relative line widths, assume the values 1.30 (**12**), 1.41 (**7**), and 2.50 (**8**), respectively.³⁰ This gradation parallels the increase in the molecular radius of the equivalent rotating sphere as expected from Kivelson's treatment, which assesses the contributions motional modulation of the anisotropic \mathbf{g} tensor and the nuclear electronic hyperfine tensor add to

the line widths in fluid solution.³¹ The finding that—contrary to expectation based on a longer correlation time of tumbling motion—proton hyperfine structure is partially resolved for **8** as opposed to **7** is due to the inequivalence of the coupling constants $a(^1\text{H})$ for the ortho, meta, and para positions in **7**. Whereas peripheral substitution on an undistorted bis(arene)[$\text{M}(\text{d}^5)$] complex usually effects changes in the spin densities that are too small to raise the equivalence of the ring protons,³² proton hyperfine splitting reacts in a very sensitive way to tilting the sandwich structure.⁹ In the case of **7**, the ensuing increase in the number of overlapping lines therefore is responsible for the fact that, for each component $m_I(^{51}\text{V})$, only an envelope of the proton hyperfine pattern is observed.

Experimental Section

All manipulations were carried out under an atmosphere of dry prepurified nitrogen. The hydrocarbon solvents were dried by refluxing over CaH_2 and then K. They were freshly distilled prior to use. Instrumental analysis: ${}^1\text{H}$ and ${}^{13}\text{C}$ NMR, Bruker AC 300 (300.1 and 75.5 MHz, respectively) and Bruker AM-400 (400.1 and 100.6 MHz, respectively) (NMR measurements were performed on solutions in sealed tubes; the solutions usually were tempered (70 °C, ~12 h) prior to recording the spectra in order to destroy complex radical cations adventitiously present); MS, Varian MAT, CH7A (EI, 70 eV); EPR Varian E12, (X-band); cyclic voltammetry, AMEL 552 potentiostat, 566 function generator, and 563 multipurpose unit, Nicolet 2090-1 digital storage oscilloscope, Kipp and Zonen BD 90 X/Y recorder, working electrode glassy carbon, counter electrode Pt wire, reference electrode saturated aqueous calomel coupled to the sample solution via a nonaqueous salt bridge. Cyclic voltammetry was performed under argon protection.

Crystal Structure Determination. A maroon crystal of **5** has been investigated on an X-ray four-circle diffractometer (for details see Table I). The lattice parameters were refined from 25 high-angle reflections: systematic absences $h0l$ ($h + l = 2n$) are consistent with the space group $P2_1/n$. The structure was solved by Patterson and difference Fourier syntheses and refined with use of anisotropic temperature factors for all non-H atoms. The hydrogen atoms were included at calculated positions ($d(\text{C-H}) = 96$ pm) with a common isotropic temperature factor. The resulting atomic coordinates are shown in Table II and bond lengths and angles in Table III.

Preparation of (1-6:1'-6'- η -Tetraphenylsilane)chromium (5). To a refluxing solution of bis(benzene)chromium (2.0 g, 9.6 mmol) and N,N,N',N' -tetramethylethylenediamine (3.5 mL, 23.0 mmol) in 100 mL of cyclohexane was added 23 mmol of n -butyllithium (14.4 mL of a 1.6 M solution in hexane) over 2 h. The resulting red-brown suspension was cooled to room temperature and stirred for an additional 12 h.

The reaction mixture was then cooled in an ice bath; the brown cyclohexane solution was decanted off from insoluble tan bis(1-lithiobenzene)chromium and replaced by petroleum ether. This suspension was cooled to -15 °C, and a solution of dichlorodiphenylsilane (2.2 mL, 10.6 mmol) in 20 mL of petroleum ether was added dropwise over 1 h. After slow warming (2 h) and additional stirring (18 h), the mixture was filtered over a glass frit and the red solid residue extracted with 250 mL of hot (100 °C) toluene. Slow cooling of this solution to -25 °C yielded 1.15 g of **5** as maroon rhombi (42% yield). **5** decomposes without melting at 165 °C. MS (m/z (relative intensity)): 388 (M^+ , 75), 336 (SiPh_4^+ , 42), 259 (SiPh_3^+ , 100), 182 (SiPh_2^+ , 60), 52 (${}^{52}\text{Cr}$, 13).

(31) (a) Kivelson, D. *J. Chem. Phys.* **1960**, *33*, 1094. (b) Wilson, R.; Kivelson, D. *J. Chem. Phys.* **1966**, *44*, 154. (c) Lewis, W. B.; Morgan, L. O. *Transition Met. Chem.* **1968**, *33*. (d) Hudson, A.; Luckhurst, G. R. *Chem. Rev.* **1969**, *69*, 191. (e) Chasteen, N. D.; Hanna, M. W. *J. Phys. Chem.* **1972**, *86*, 3951.

(32) Elschenbroich, C.; Möckel, R.; Zenneck, U.; Clack, D. W. *Ber. Bunsen-Ges. Phys. Chem.* **1979**, *83*, 1008.

(33) Johnson, C. K. ORTEP, A Fortran Thermal Ellipsoid Plot Program for Crystal Structure Illustrations. Report ORNL-3794; Oak Ridge National Laboratory: Oak Ridge, TN, 1965.

(29) Elschenbroich, C.; Bilger, E.; Ernst, R. D.; Wilson, D. R.; Kralik, M. S. *Organometallics* **1985**, *4*, 2068.

(30) For analogous behavior of diphenylphosphino derivatives see: Elschenbroich, C.; Stohler, F. *Chimia* **1974**, *28*, 730.

Anal. Calcd for $C_{24}H_{20}SiCr$: C, 74.23; H, 5.15. Found: C, 73.03; H, 5.27.

Preparation of (1-6:1'-6'- η -Tetraphenylsilane)vanadium (7). The synthesis of 7 proceeded in analogy to that of 5. From 1.2 g (5.8 mmol) of bis(benzene)vanadium (12) 0.78 g (2.0 mmol, 35%) of 7 was obtained as glistening black stars. 7 decomposes at 225 °C before melting. MS (m/z (relative intensity)): 387 (M^+ , 100), all fragment ions $I < 10\%$. Anal. Calcd for $C_{24}H_{20}SiV$: C, 74.73; H, 5.16. Found: C, 73.77; H, 5.48.

Preparation of Bis((triphenylsilyl)- η^6 -benzene)chromium (6). A 1.3-g (6.3-mmol) amount of bis(benzene)chromium (9) was metalated as described above. A 4.45-g (15.1-mmol) portion of chlorotriphenylsilane, dissolved in 100 mL of petroleum ether, was then added to the cooled (0 °C) suspension with vigorous stirring. Filtration followed by partial extraction of the sparingly soluble solid residue with 250 mL of boiling toluene gave 100 mg (1.4 mmol, 2.4% yield) of 6 as a yellow-orange, amorphous powder. MS (m/z (relative intensity)): 724 (M^+ , 30), 388 (M^+ - $SiPh_4$, 100), 336 ($SiPh_4^+$, 25), 259 ($SiPh_3^+$, 75), 182 ($SiPh_2^+$, 40), 52 (^{62}Cr , 25). Anal. Calcd for $C_{48}H_{40}Si_2Cr$: C, 79.55; H, 5.52. Found: C, 79.65; H, 5.43.

Preparation of Bis((triphenylsilyl)- η^6 -benzene)vanadium (8). The synthesis of 8 was performed as described for the chromium analogue 6. From 0.79 g (3.8 mmol) of bis(benzene)vanadium (12) 0.24 g (0.33 mmol, 8.7%) of 8 was obtained as maroon microcrystals. MS (m/z (relative intensity)): 723 (M^+ , 17), 387 (M^+ - $SiPh_4$, 38), 336 ($SiPh_4^+$, 49), 259 ($SiPh_3^+$, 100), 182 ($SiPh_2^+$, 62). Anal. Calcd for $C_{48}H_{40}Si_2V$: C, 79.64; H, 5.57. Found: C, 79.10; H, 5.88.

Cocondensation of Tetraphenylsilane with Chromium Atoms. A 1-g (3-mmol) amount of tetraphenylsilane (internal vaporization) and 0.52 g (10 mmol) of chromium were cocondensed at -196 °C (10^{-4} mbar) over 1 h. Extraction of the reaction mixture with toluene followed by removal of solvent under reduced pressure yielded an orange solid. According to 1H NMR spec-

troscopy this material consists of a mixture of tetraphenylsilane and bis((triphenylsilyl)- η^6 -benzene)chromium (6) in an approximate 20:1 ratio. No traces of 5 were found.

Protodesilylation of (1-6:1'-6'- η -tetraphenylsilane)chromium (5). A 50-mg amount of 5 (0.13 mmol) was dissolved in 50 mL of warm THF, giving a clear red-orange solution. To this was added 2.5 mL of N_2 -saturated water. Within minutes, the solution turned yellow. Filtration through activated alumina and removal of solvent under reduced pressure, followed by recrystallization from ligroin, yielded 20 mg of a light tan powder, which was subjected to 1H and ^{13}C NMR and mass spectral analysis. MS (m/z (relative intensity)): 794 (10^+ , 17). 1H NMR (C_6D_6): δ 7.85 (doublet of doublets, relative intensity 1), 7.71 (doublet of doublets, 4.2), 7.20 (m, 12), 4.23 (s, 6.5). ^{13}C NMR (C_6D_6): δ 136.9 (C_{meta}), 134.8 (C_{para}), 130.9 (C_{ipso}), 129.9 (C_{meta}), 74.8 (9). From this analysis, it is apparent that the product is a mixture of primarily bis(benzene)chromium (9), poly(diphenylsiloxane), and traces of 10.

Acknowledgment. We thank the Deutsche Forschungsgemeinschaft (DFG) and the donors of the Fonds der Chemischen Industrie for the support of this work. J.H. is indebted to Deutscher Akademischer Austauschdienst (DAAD) for the award of a scholarship.

Registry No. 5, 125594-40-3; 6, 125594-41-4; 7, 125594-42-5; 8, 125594-43-6; 9, 1271-54-1; 11, 1048-08-4; 12, 12129-72-5; Cr, 7440-47-3; Ph_2SiCl_2 , 80-10-4; Ph_3SiCl , 76-86-8; bis(1-lithio-benzene)chromium, 125594-39-0; poly(diphenylsiloxane), 775-12-2.

Supplementary Material Available: A table of anisotropic temperature factors and atomic coordinates of the H atoms and a complete list of bond lengths and angles (3 pages); a table of the structure factors (9 pages). Ordering information is given on any current masthead page.

Theoretical Study of $Cp_2Ti(H)(SiH_3)$ and Cp_2TiSiH_2 and Their Possible Role in the Polymerization of Primary Organosilanes

John F. Harrod,[†] Tom Ziegler,^{*‡} and Vincenzo Tschinke[‡]

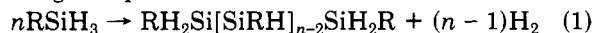
Departments of Chemistry, McGill University, Montreal, Quebec H3A 2K6, Canada,
and University of Calgary, Calgary, Alberta T2N 1N4, Canada

Received May 11, 1989

The two reactions $Cp_2Ti(H)(SiH_3) \rightarrow Cp_2Ti=SiH_2 + H_2$ and $Cp_2Ti=SiH_2 + SiH_4 \rightarrow Cp_2Ti(H)SiH_2SiH_3$ have been modeled with use of density functional theory and the HFS-LCAO program system by Baerends et al. Both kinetic and thermodynamic features of these reactions were studied, and the results of the computations indicate that the first reaction can proceed with a moderate activation barrier of ca. 60 kJ mol⁻¹ and an enthalpy of ca. 40 kJ mol⁻¹. The second reaction is found to be exothermic (ca. -48 kJ mol⁻¹) with an activation barrier of ca. 12 kJ mol⁻¹. The previously proposed mechanism for the titanocene-catalyzed dehydrocoupling of organosilanes is evaluated in terms of these calculations, and it is concluded that the α -hydride elimination-silane addition route is viable. The structural and thermodynamic parameters for each of the important reaction intermediates are also calculated.

I. Introduction

It has recently been shown that the polymerization of primary organosilanes¹ can be catalyzed by dehydrocoupling under the influence of titanocene-based catalysts, according to eq 1.



This reaction is close to thermodynamically neutral. The enthalpy for the elementary dimerization reaction

$$RSiH_3 + R'SiH_3 \rightarrow RH_2SiSiH_2R' \quad (2)$$

can be estimated with use of literature bond energy values² as

$$\begin{aligned} \Delta H_2 &= 2[D(Si-H)] - D(H-H) - D(Si-Si) \\ &= (786 - 432 - 340) \text{ kJ mol}^{-1} = 14 \text{ kJ mol}^{-1} \end{aligned}$$

(1) (a) Aitken, C.; Harrod, J. F.; Samuel, E. *J. Organomet. Chem.* **1985**, *279*, C11. (b) Aitken, C.; Harrod, J. F.; Samuel, E. *J. Am. Chem. Soc.* **1986**, *108*, 4059. (c) Harrod, J. F.; Yun, S. S. *Organometallics* **1987**, *6*, 1381. (d) Aitken, C.; Harrod, J. F.; Samuel, E. *Can. J. Chem.* **1986**, *64*, 1677. (e) Aitken, C.; Harrod, J. F.; Gill, U. S. *Can. J. Chem.* **1987**, *65*, 1804. (f) Harrod, J. F. *ACS Symp. Ser.* **1988**, *No. 360*, 89. (g) Harrod, J. F. In *Transformation of Organometallics into Common and Exotic Materials: Design and Activation*; Laine, R. M., Ed.; NATO ASI Series, Series E, No. 141; Kluwer: Boston, MA, 1988; p 103.

[†] McGill University.

[‡] University of Calgary.